2015

In Planta Production of Flock House Virus Transencapsidated RNA and Its Potential Use as a Vaccine

Yiyang Zhou

Payal D. Maharaj
Touro University California, payal.maharaj@tu.edu

Jyothi K. Mallajosyula
Touro University California, jyothi.mallajosyula@tu.edu

Alison A. McCormick
Touro University California, alison.mccormick@tu.edu

Christopher M. Kearney

Recommended Citation

Zhou, Y., Maharaj, P., Mallajosyula, J., McCormick, A., & Kearney, C. (2015). In planta production of flock house virus transencapsidated RNA and its potential use as a vaccine. Molecular Biotechnology, 57(4), 325-336.

In planta production of *Flock House virus* trans-encapsidated RNA and its potential use as a vaccine

Yiyang Zhou[a], Payal D. Maharaj, Jyothi K. Mallajosyula, Alison A. McCormick[b], Christopher M. Kearney[a,c]#

Biomedical Studies Program[a] and Department of Biology[c], Baylor University, Waco, Texas, USA;

Touro University California, College of Pharmacy, Vallejo CA, USA[b]

Running Head: *In planta* transencapsidated Flock House virus nanoparticle

#Address correspondence to Christopher Kearney, chris_kearney@baylor.edu

Key words: Nanoparticle; Vaccine; Flock house virus; Tobacco mosaic virus; Plant

Abstract: 170 words

Text (excluding references and figure legends): 4609

Abstract:

We have developed a transencapsidated vaccine delivery system based on the insect virus, *Flock House virus* (FHV). FHV is attractive due to its small genome size, simple organization, and non-pathogenic characteristics. With the insertion of a *Tobacco mosaic virus* (TMV) origin of assembly (Oa), the independently replicating FHV RNA1 can be transencapsidated by TMV coat protein. In this study we demonstrated that the Oa adapted FHV RNA1 transencapsidation process can take place *in planta*, by using a bipartite plant expression vector system, where TMV coat protein is expressed by another plant virus vector, *Foxtail mosaic virus* (FoMV). Dual infection in the same cell by both FHV and FoMV was observed. Though an apparent classical coat-protein-mediated resistance repressed FHV expression, this was overcome by delaying inoculation of the TMV coat protein vector by three days after FHV vector inoculation. Expression of transgene marker in animals by these *in vivo* generated transencapsidated nanoparticles was confirmed by mouse vaccination, which also showed an improved vaccine response compared to similar *in vitro* produced vaccines.

Introduction

Virus-based nanoparticles have been extensively explored as a vaccine delivery strategy due to their typically higher immunogenicity compared with unassembled vaccine antigens (1, 2), their potential to serve as their own adjuvant (1-3), and their greater safety and potentially relatively lower cost of protection compared to traditional vaccines(4). Virus-like particles (VLPs) display vaccine antigen on their surface and can be produced by the self-assembly of viral coat protein subunits expressed in a heterologous host, such as bacteria (5) or plants (6), or in mammalian cells (7). An alternative to VLPs is to use viral coat protein to encapsidate the RNA of another virus, with the RNA expressing the vaccine antigen once delivered to the target cell. In this way, the viral RNA can be packaged in an especially resistant nanoparticle similar to a VLP. The potential advantage of this strategy over VLPs is the activation of innate immunity by viral replication (8-10).

Among numerous trials using viral nanoparticles for antigen delivery, *Tobacco mosaic virus* (TMV) nanoparticles seem to hold special promise. TMV virions are characterized by great stability and low cost production (11), and a recent study suggests that the human population has already been extensively exposed to TMV coat antigen through exposure to food and tobacco sources (12). Furthermore, extensive data show that pre-existing immunity to TMV coat does not disrupt boosting of either cytotoxic T lymphocyte (CTL, (13, 14)

or antibody target antigens (15, 16). Lastly, TMV virions are extremely stable, remaining infective for over a century at room temperature (17). TMV exhibits robust expression in plants at up to 5-10% dry weight, and is easy to purify at the commercial scale (11).

Consequently, TMV nanoparticles have been explored as a VLP epitope platform. The highly uniform repeated organization of 2130 copies of coat protein subunits and the associated strong cross-linking pattern provide greatly improved efficacy to deliver antigens to antigen presenting cells. Various studies have validated that TMV-antigen conjugation can induce B cell activation and raised antibody titers (15, 18, 19), even when the conjugates are poorly immunogenic, such as carbohydrates (20). Furthermore, TMV uptake by dendritic cells is rapid and efficient (14, 18), and peptide-presenting TMV nanoparticles were proven to be able to elicit T cell responses with augmented interferon gamma (IFN γ) levels (14). We have also previously successfully tested ovalbumin-conjugated TMV vaccines, as well as a bivalent TMV vaccine displaying both mouse melanoma-associated CTL epitopes p15e and tyrosinase-related protein 2 (Trp2) peptides (13). Immunization resulted in a significantly improved survival after lethal tumor challenge. A recent study also demonstrated TMV's great potential to be used in stand-alone or prime-boost dendritic cell activation strategies (18).

In addition to utilizing TMV as a VLP to present surface epitopes, development has also proceeded with TMV coat protein encapsidated RNA vaccines. In previous experiments, we have produced and tested Semliki Forest virus (SFV) RNA encapsidated with TMV coat protein *in vitro*. Attenuated SFV was modified by insertion of a TMV origin of assembly to produce, *in vitro*, rod shaped virus particles that resembled TMV (21) by mixing SFV-Oa RNA with purified TMV coat protein. Vaccination with SFV-Oa encoding the model antigen beta-galactosidase (bGal) resulted in boosted antibody responses to bGal protein, demonstrating that TMV encapsidated RNA was translated and was antigenic in the absence of adjuvant, and, further, that the presence of the TMV Oa did not disrupt SFV replication functions. However, as a common phenomenon of pathogenic RNA virus vaccines (22), SFV-Oa RNA induced apoptosis in infected cells, which may limit duration of antigen exposure and reduce immune activation to transgene encoded antigens.

To improve on our previous results with SFV, we applied TMV encapsidation to the RNA of the nonpathogenic insect virus, *Flock House virus* (FHV), which is capable of replicating in human cells. The advantages of FHV include a bipartite genome, where the polymerase is encoded by the independently replicating RNA 1 and the structural capsid gene is encoded by RNA 2, allowing for easy manipulation of the RNA1 genome for vaccine development

and the separation of replication from packaging. We have already tested *in vitro* assembled TMV-FHV particles and have shown that TMV Oa did not disrupt FHV viral replication, using an enhanced green fluorescent protein (eGFP) transgene to monitor replication and expression in mammalian cells (23). However, the limitations of *in vitro* encapsidation remain with this system; namely the cost of RNA synthesis and potentially reduced translation due to inefficient *in vitro* 5' capping.

To overcome these limitations, we explored an *in planta* strategy for producing viral RNA *in vivo*. For the present study, we hypothesized that FHV RNA, which replicates well in mammalian (24) and plant cells (25) but is not a pathogen of either, could be encapsidated *in planta* if sufficient TMV coat protein were provided *in trans*. We further predicted that *in planta* produced nanoparticles would be able to express transgene after animal vaccination, and will be comparatively more immunogenic than *in vitro* nanoparticles due to natural 5' capping. As described in the following report, we used a 35S promoter to express FHV-eGFP-Oa RNA and the plant viral vector Foxtail mosaic virus (FoMV) to express TMV coat protein in quantities sufficient for encapsidation of FHV RNA in agroinoculated *Nicotiana benthamiana* plants. Replication of functional FHV-eGFP-Oa was observed as an unusually strong eGFP fluorescence, and near wild type levels of TMV-coat protein were produced by co-delivered FoMV vector. We observed virion particles of the

typical TMV morphology as a final product. When these nanoparticles were used to vaccinate mice, the expression of eGFP transgene was confirmed by an anti-eGFP immune response greater than that observed for *in vitro* encapsidated control particles. This is the first report of *in planta* transencapsidated nanoparticles and represents the first step towards producing a commercially viable vaccine of this type.

MATERIALS AND METHODS

Construction of T7/FHV-C2-GFP vector and expression in mammalian cells. The plasmid containing the FHV RNA1 expression cassette was kindly provided by Dr. A. Ball. It is a T7 promoter-driven plasmid containing the RNA1 portion of the FHV genome and was previously described (26). A polylinker, CTCGAGGCGATCGCCTGCAG, encompassing the 3 restriction sites XhoI, AsiSI and PstI, was cloned into one of four insertion sites: C1, nt. 3034; C2, nt. 3037; C3, nt. 2731; and C4, nt. 3055, and confirmed by direct sequencing. Enhanced green fluorescent protein (eGFP) ORF was then cloned into these sites via XhoI and PstI to create T7/FHV-C-(1-4)-GFP constructs (Fig. 1A). To confirm stability of the eGFP modified FHV viral RNA, full-length RNA transcripts were generated from the T7/FHV-C-GFP DNA *in vitro* via a T7 promoter kit (mMESSAGE mMACHINETM, Ambion, TX). 2 µg RNA was used to transfect BHK-21 cells with DMRIE-C (Invitrogen, Carlsbad, CA). Transfected cells were incubated at 37°C for 4 hours, after which fresh

156 growth media was used to replace transfection media. Cells were then placed
157 at 28°C for 24 hours. Expression of fluorescence was confirmed using a
158 Nikon Eclipse TS100 microscope and NIS-elements imaging software. Cells
159 were observed for 2 days post-transfection.
160
161 ***In planta* expression vectors.** In order to express FHV in plants, full-length
162 FHV viral vector sequence was transferred from T7/FHV-C2-GFP (Fig. 1A)
163 and placed between the StuI/XbaI sites of the plant binary vector JL22 (27) to
164 create 35S/FHV-C2 (Fig. 2A). To allow Oa insertion, additional restriction
165 sites were introduced on either side of the eGFP ORF by amplifying the eGFP
166 ORF with an upstream primer containing XhoI/AscI and a downstream primer
167 containing AvrII/PstI and then reinserting this product into 35S/FHV-C2
168 between the XhoI and PstI sites. TMV Oa (95 bp: TMV nts. 5432-5527; (28)
169 was inserted upstream or downstream of the eGFP ORF to create
170 35S/FHVC2-o1 and -o2, respectively (Fig. 2A). PCR with a primer containing
171 a mutated eGFP ORF stop codon was used to create 35S/FHVC2-o3.
172
173 Several modifications were made to improve eGFP expression. T7/FHV-C4-
174 2sg was created to maintain B2 expression, by duplicating the 3' end of FHV
175 RNA1 (nt. 2518-3055) and inserting it after the eGFP open reading frame in
176 T7/FHV-C4-GFP. 35S/FHV-C4-2sg (Fig. 2B) was generated by transferring
177 the viral sequence into JL22 (27), as outlined above. To express both FHV B2

and eGFP separately, a 498 bp DNA segment was synthesized (gBlock, IDT, Coralville, IA) and inserted between the XhoI and PstI sites in 35S/FHV-C4. This segment contained a stop codon in the B2 ORF, 10 bp of the FHV 3' UTR for any potential required context for B2 ORF expression, the 95 bp TMV Oa, a repeat of the presumed B2 subgenomic promoter (FHV 2480-2809, including 69 bp past the B2 start) to drive eGFP expression, and a start codon and insertion sites for eGFP. To recreate a more FHV authentic 3' region following the eGFP ORF, the final 24 bases of B2 ORF was added downstream of the eGFP stop codon, to yield the final construct: 35S/FHV2sg2 (Fig. 2B). All recombinant DNA methods and suppliers for the plant constructs were as previously described (29).

Agroinoculation and visualization. *Nicotiana benthamiana* plants were grown and agroinoculated as previously described (29). Excised eGFP-fluorescent leaves were visualized using a blue light Dark Reader (Clare Chemical, Dolores, CO, USA). The defective interfering construct DI638/wtGFP (30) was a gift from A. Rao (UC Riverside) and those inoculations were visualized with a hand held UVL-56 lamp (UVProducts, Upland, CA, USA).

Relative fluorescence resulted by different FHV constructs was measure by grinding inoculated leaf tissue in 1X Phosphate Buffered Saline (PBS). The

collected supernatant was assessed on a microplate reader (Thermo Fluoroskan Ascent FL), with black 96 well plate (COSTAR 3925, Corning Inc. NY). Filter set of 485nm (excitation) and 538nm (emission) was used in order to detect eGFP fluorescence.

Plant protoplasts. Protoplasts were prepared from *N. benthamiana* leaves 4 days post-inoculation. Leaves were sliced into 2 mm strips and vacuum infiltrated with MMC buffer (13% mannitol, 5 mM MES, 10 mM $CaCl_2$, pH 5.8) containing 1% Onozuka cellulase RS and 0.5% Macerase (both from Phytotechnology Labs, Shawnee Mission, KS, USA) and gently rocked overnight. Protoplasts were mounted in MMC on a glass slide. Images were obtained as previously described (29).

Plant produced nanoparticles. To purify nanoparticles, agroinoculated *N. benthamiana* leaves, 4-7 days p.i., were ground in a mortar in extraction buffer (50 mM sodium acetate, 0.86 M NaCl (5% w/v), 0.04% sodium metabisulfite, pH 5.0). Crude homogenate was filtered through cheesecloth and 8% (v/v) n-butanol was added, and then incubated at room temperature for 15 min, and then centrifuged at 10,000 x g for 15 min. The supernatant was decanted through cheesecloth, and nanoparticles were precipitated with PEG 8000 (EMD Millipore, USA) at 4% on ice for 1 hr, followed by centrifugation at 10,000 x g for 10 min. The pellet was resuspended in a

minimum of 10 mM phosphate buffer (pH 7.2) and then centrifuged at 16,000 x g for 10 min. The supernatant was collected and nanoparticles were purified with an additional round of PEG precipitation. The final nanoparticle pellet was suspended in 10mM phosphate buffer (pH 7.2) and stored at -20°C. Protein concentration was determined by bicinchoninic acid (BCA) assay (Pierce Biotechnology, Rockford, IL, USA).

Transmission electron microscopy was used to visualize purified nanoparticles on a JEOL JSM 1010 microscope. A 3 µl drop of nanoparticles was adsorbed onto 300 mesh formvar coated grids (Electron Microscopy Sciences, PA, USA) for 1 minute, drawn off, and stained with 1% phosphotunstic acid (pH 7). Image was taken by XR16 TEM camera (Advanced Microscopy Techniques, MA, USA), and with AMT Image Capture Engine V602 (Advanced Microscopy Techniques, MA, USA), at 30,000X to 40,000X magnification.

***In vitro* nanoparticle assembly and vaccine preparation.** SFV-eGFP or FHV-eGFP RNA was transcribed from T7 plasmids using a capped RNA synthesis kit (MmessageMachine; Ambion), quantitated by absorbance, and checked for integrity by gel electrophoresis. 50 µg of RNA was then incubated with 1.4 mg of TMV coat protein, prepared by a modified protocol as previously described (21). Briefly, encapsidations were carried out using

overnight incubation in a 0.05 M phosphate buffer (pH7) at room temperature. Particles were recovered by PEG precipitation and quantitated by BCA assay (BioRad, CA).

Vaccination and immune response evaluation in mice. BALB/c mice (Charles River, CA) were housed at Touro University according to guidelines established in the Care and Use of Animals, and performed according to IACUC approved protocols. Typically, 3 mice were given a 100 – 200 µl subcutaneuous (s.c.) injection of 15 or 30 µg encapsidated product, or 15 µg eGFP protein as a positive control (Vector Labs), or PBS as a negative control. Vaccines were typically administered at two-week intervals and tail vein bleeds were taken at 10 days after vaccines 2 and 3 for enzyme linked immunosorbent assay (ELISA) analysis.

The IgG immune response was determined by ELISA. 96-well microtiter plates (MaxiSorp; Nalge Nunc) were coated with 5 µg/ml eGFP protein (Vector Labs) in 50 mM carbonate/bicarbonate buffer (pH 9.6). After blocking with 2% bovine serum albumin (BSA) in PBS, serial dilutions of the sera were added for one hour, the plates were washed and incubated for an additional hour with anti-mouse IgG Horse Radish Peroxidase (HRP) conjugated secondary antibody (Southern Biotech) in PBS+BSA. Plates were developed using a tetramethyl benzidine substrate solution (TMB; BioFx) and the

reactions were stopped by the addition of 1N sulfuric acid. Plate absorbance was read at 450 nm in a 96-well plate spectrophotometer (Molecular Devices). Relative anti-eGFP titers reported were determined from a standard curve generated by a 3-fold serial dilution of a 100 ng/ml rabbit anti-eGFP polyclonal antibody (Sigma) detected with an anti-Rabbit-HRP secondary. Statistical analysis was carried out using Prism software (GraphPad), using unpaired t-test with Welch's correction.

RESULTS

FHV vector expression in mammalian cells. FHV vectors were designed and tested for the expression of eGFP in BHK-21 cells. A cassette containing three restriction sites (XhoI, AsiI and PstI) was placed at the FHV C2 site (31); namely, immediately downstream of the polymerase/B1 stop codon, which is also six codons upstream from, and in phase with, the B2 stop codon (Fig. 1A). This FHV-C2 construct thus expresses a B2-eGFP-B2 fusion, with 99 amino acids of B2 upstream of eGFP and 6 amino acids of B2 at the C terminus. Insertion at a second eGFP ORF insertion site, the C4 site, would produce the full B2 protein fused to the eGFP (Fig. 1A). eGFP expression was observed in mammalian cells (Fig. 1B) within 24 hours post transfection. Expression with both constructs peaked at 48 hours and was maintained until 72 hours, with approximately 15-20% transfection efficiency. Fluorescence

287 began to decrease after 72 hours and gradually diminished over time. The C4
288 insertion construct gave reduced fluorescence compared to C2 (Fig. 1B).
289
290 **Strong FHV/eGFP expression in *N. benthamiana* after p19 co-**
291 **agroinoculation.** The 35S/FHV-C2-GFP and 35S/FHV-C4-2sg constructs
292 were made by transferring viral sequences from the mammalian vectors into
293 plant binary vector pJL22 (27) between a cauliflower mosaic virus 35S
294 promoter and 35S terminator (Fig. 2). Leaves agroinoculated with these
295 constructs gave a weak fluorescence (Fig. 3), as did leaves inoculated with
296 the positive FHV/wtGFP control, F1DI, comprising FHV RNA1 and DI638, the
297 defective interfering RNA of FHV RNA2, carrying wtGFP (30). However, when
298 the silencing suppressor, p19 (32), was provided by co-agroinoculation, a
299 much stronger fluorescence was observed (Fig. 3) which was much stronger
300 than the F1DI + p19 control. Subsequently, p19 was included in all
301 inoculations.
302
303 To create a FHV vector competent for encapsidation by TMV CP, the TMV
304 Oa was inserted into 35S/FHV-C2-GFP at two different positions (35S/FHV-
305 C2-o1, o2), and adjacent to eGFP ORF. In order to test the influence of C
306 terminal TMV Oa fusion on eGFP expression, a third construct, 35S/FHV-C2-
307 o3, was designed with the introduction of a stop codon at the natural stop site
308 of eGFP, resulting in an eGFP fusion with B2 only at the N terminus. These

three Oa containing constructs (35S/FHV-C2-o1 to o3) were found to express only slightly less eGFP in leaves than the non-Oa, 35S/FHV-C2 (Fig. 3 and Fig. 4A). This was unexpected since the TMV Oa sequence was added close to either the putative sub-genomic promoter or the FHV 3'UTR. Little difference in fluorescence was observed between the three Oa containing constructs.

To express the FHV silencing suppressor, B2 (Albariño et al., 2003), in conjunction with eGFP, we made variants of 35S/FHV-C4-2sg. To prevent the deletion of the eGFP ORF, we placed the eGFP ORF at the 3' terminus of the virus, in contrast to the C4-2sg construct. Any homologous recombination between the two homologous subgenomic regions would delete B2 and Oa, but not eGFP, and deletion mutants would not be packaged as nanoparticles. It was observed that the 35S/FHV-C2-GFP construct clearly resulted in a brighter fluorescence than 35S/FHV-C4-2sg, which was further confirmed by fluorometry analysis (Fig. 4A).

To explore the impact of improved B2 expression, a portion of the FHV 3' UTR, which is normally downstream of the B2 ORF, was added to the internal B2 ORF followed by the TMV Oa. The final construct 35S/FHV2sg2 was created by adding 24 bp of C-terminal B2 sequence to aid eGFP expression by providing more natural context at the 3' end of the ORF. We expected to

see stronger eGFP expression and/or FHV B2 expression that would functionally replace p19. However, the FHV2sg2 vector did not significantly improve eGFP fluorescence expression compared with the original C4-2sg construct *in planta* (Fig. 3). Other constructs were built and tested, which included the precedent construct of FHV2sg2 (data not included) and a vector with the addition of strong Kozak context in pursuit of enhanced expression (FHV2sg2KSS, supplementary Fig 1a). Neither resulted any improvement in eGFP fluorescence (Fig 3). In all cases, p19 was still required via co-agroinoculation for strong fluorescence. All subsequent experiments used the 35S/FHV-C2-o3 construct co-agroinoculated with p19.

Co-expression of FHV and FECT in plants

To encapsidate FHV vector RNA *in planta*, a ratio of 20:1 mass ratio of TMV coat protein (CP) to RNA is required. The high expression *Foxtail mosaic virus* vector, FECT (29), was used to produce TMV CP without being itself encapsidated. FECT produced TMV CP at a level comparable to the TMV vector JL24 (27), which expresses TMV CP as a native gene (Fig. 5).

We next examined the ability of FHV and FECT to co-infect cells, to ensure there was no replication interference. In a co-infection test system, 35S/FHV-C2 expressing eGFP and FECT expressing DsRed were co-agroinoculated into several leaves, resulting in a yellow-green fluorescence under blue light

353 when viewed without magnification (Fig. 6A). In order to determine co-
354 infection of single cells, co-infected leaves were reduced to protoplasts and
355 the protoplasts were examined under a UV microscope. As seen in a
356 representative photo (Fig. 6B), about 75% of the eGFP positive cells are also
357 DsRed positive, but not vice versa. FECT strongly infects the great majority of
358 plant cells (29), as seen by the DsRed signals in Fig. 6B. FHV/eGFP is an
359 insect virus construct and infects a much smaller number of plant cells, but
360 those that are infected are mostly co-infected with FECT/DsRed,
361 demonstrating the high frequency at which double infection occurs with this
362 system, given the limitations of FHV infectivity itself.
363
364 **eGFP expression by FHV enhanced by delayed TMV CP expression**
365 Nanoparticles were produced by agro-inoculation with 35S/p19, 35S/ FHV-
366 C2-o3, and 35S/FECT-TMVCP. The average size of our FHV-C2-o3
367 nanoparticles is estimated to be ~200nM based on the length of the FHV RNA
368 genome (C2-o3; 4182 nts.), compared with wide type TMV (6395 nts.) that
369 generates a 300nM particle (Fig. 7).
370
371 In all experiments, the presence of TMV CP at the time of FHV early infection
372 (i.e., co-inoculation) led to reduced eGFP fluorescence. We hypothesized that
373 CP binding the Oa early in infection impeded the replicative or translational
374 events of FHV RNA. To test this, a “2-step” protocol was used in which the

375 FECT/TMV CP inoculation was delivered three days after the FHV/GFP/Oa
376 and p19 inoculations. The 2-step procedure consistently increased eGFP
377 expression (Fig. 4).
378
379 **Immune response to nanoparticles in mice**
380 In order to test the capacity of transencapsidated FHV RNA to express the
381 eGFP transgene in mice, *in planta* transencapsidated FHV RNA was used to
382 immunize BALB/c mice with *in vitro* transencapsidated FHV RNA or SFV RNA
383 as encapsidation controls. Two doses of 15 µg or 30 µg encapsidated RNA
384 (0.75 or 1.5 µg of RNA, respectively) were given by subcutaneous injection,
385 without adjuvant. eGFP protein (15 µg) was used as a positive control while
386 PBS buffer was used as a negative control. Sera collected from mice before
387 immunization and after a single dose were essentially negative for immune
388 responses for all groups (data not shown). Weak but detectable anti-eGFP
389 IgG responses were measured by ELISA after a second vaccination (pV2,
390 Fig. 8), but all groups were statistically similar to PBS, including eGFP protein
391 immunization. After a third immunization (pV3), all groups showed a strong
392 trend toward augmented immunity against eGFP, but in large part were not
393 significantly different than PBS, mainly due to high variance between
394 responders and small group size. However, the highest dose of *in planta*
395 encapsidated FHV (C2-o3, 30µg) and eGFP protein control had IgG titers
396 significantly higher than all *in vitro* encapsidated viral vector treatments. This

confirmed the successful expression of eGFP transgene by transencapsidated FHV RNA, after uptake and presumed co-translational disassembly of TMV coat protein. This is notable, in light of low replication ability of FHV RdRp in animal cells at 37 degree (33).

Discussion

We have shown in this study that FHV can be encapsidated *in planta* with TMV coat protein and the resulting nanoparticle vaccines had improved characteristics compared to *in vitro* encapsidated FHV RNA. In previous studies, we demonstrated that SFV could be encapsidated *in vitro* with TMV coat protein (21). TMV coat protein produced *in vivo* had also been used to assemble wild type TMV virions in *E. coli* (34) and mRNAs had been encapsidated *in planta* to form TMV hybrid virions (35). As well, *Brome mosaic virus* (BMV) RNA containing the TMV Oa was transencapsidated with TMV CP in barley protoplasts (36) and Rao and colleagues produced non-specific transencapsidated virions by coat protein of the similarly structured BMV in studying encapsidation specificity (37). Though FHV virions use a multitude of molecular cues in virion assembly, similar to other icosahedral viruses (38), TMV and other tobamoviruses utilize a single Oa sequence to initiate assembly, with the remainder of the encapsidated sequence apparently without further molecular cues (39). Thus, any RNA containing the TMV Oa should be able to be transencapsidated. It may be possible to extend

this technique to other viral species for viral-vectored nanoparticle vaccine assembly *in planta*.

The individual components of the nanoparticles appeared to be produced at high levels. The FECT viral vector produced TMV CP at the same level as the native TMV vector, JL24(Fig 5). FHV vector levels, as measured by visually assessed fluorescence of eGFP (Fig. 3), were greater in side by side studies than the DI638 vector used in previous FHV work in *N. benthamiana* (37). The coexpression of p19 silencing suppressor further boosted this eGFP expression even with FHV vector constructs that had an intact B2 silencing suppressor (Fig.2 and 3).

As a prerequisite for assembly, coexpression of both vectors in a single cell is necessary. The FECT vector was shown to express in the majority of cells harboring the FHV vector (Fig. 6). However, when FHV RNA and TMV CP vectors were co-inoculated, we saw a significant decrease in fluorescence. A supplementary experiment was performed in order to exclude the possibility of FECT interfering FHV replication (suppl. Fig. 2). This inhibition phenomenon is most likely mediated by classical coat protein resistance (40) and was previously observed by the Ahlquist group working with BMV transencapsidated by TMV CP. BMV RNAs 1 and 2 containing the TMV Oa decreased in replication 20-fold when co-inoculated with BMV RNA 3

441 expressing TMV CP (36). This was theorized to be due to TMV CP binding to
442 the BMV RNAs and interfering with replication. We investigated this
443 hypothesis by separating the agroinoculation of FHV vector and TMV CP into
444 two steps, delaying the expression of TMV CP until FHV RNA replication was
445 sufficient to generate robust eGFP protein. The two-step plants consistently
446 showed higher expression of the viral eGFP transgene (Fig. 4), suggesting
447 RNA packaging by TMV CP reduced FHV RNA replication and/or translation.
448
449 Several modifications were made in an attempt to improve FHV vector
450 replication in plants. The addition of TMV Oa led to strong inhibition of BMV
451 RNA replication even in the absence of TMV CP in a previous study (36).
452 However, we observed only a slight decrease in eGFP production by the FHV
453 vectors carrying Oa. C2 constructs carrying Oa at two different sites (C2-o1
454 and C2-o2) did not differ significantly in eGFP fluorescence produced.
455 Recreating a native C-terminus for eGFP (C2-o3) also had no effect.
456 Constructs with unmodified B2 silencing suppressor ORFs (2sg2 series) were
457 less effective than the C2 series with the B2 ORF fused to eGFP. These were
458 longer constructs, but the shorter C4 construct was also less fluorescent in
459 mammalian cells than the C2 construct (Fig. 1B), suggesting the common C4
460 insertion site as detrimental. Ultimately, the inclusion of p19 as a co-inoculant
461 was the sole factor in achieving high eGFP expression in plants from the FHV
462 vectors, re-confirming the importance of mitigating RNA silencing *in planta*.

463

464 It is possible that the size of the duplicated subgenomic promoter in the 2sg2
465 series was insufficient since a longer FHV subgenomic promoter segment
466 was found more efficacious in a previous study (41). Beyond the core nts.
467 2518-2777, the region from nt. 2302-2518 may serve as an important
468 enhancer (42). Polarity preference was found on FHV (41) and other positive-
469 strand RNA viruses; specifically, that two pieces of sgRNA were replicated at
470 different levels, with the longer one (closer to replicase) being dominant. This
471 may explain why we see more eGFP fluorescence in the 35S/ FHV-C4-2sg,
472 which has the eGFP ORF included in the first sgRNA3, than–FHV-2sg2
473 series, which have eGFP ORF included in the second sgRNA3.

474

475 In order to verify the capacity of these transencapsidated nanoparticles to
476 express transgene in animal cells, FHV C2-o3 encapsidated particles were
477 used as a vaccine, and an IgG antibody response to eGFP was measured
478 (Fig. 8). Despite the reported deficiency of FHV replicase to function well in
479 37 degree (33), a titer of anti-eGFP antibody equal to that of 15ug eGFP
480 protein was observed after three injections with 30 ug of FHV C2-o3
481 nanoparticles (1.5ug FHV RNA). This demonstrated delivery and expression
482 of the eGFP transgene and suggested a considerable boosting of the immune
483 response by RNA antigen delivery. *In vitro* FHV and SFV/TMV CP
484 nanoparticles produced a significantly lower immune response in this study,

possibly due to lower percentage of 5' capping, which is known to affect translation efficiency.

During nanoparticle *in planta* assembly, FHV subgenomic RNA3 may also be encapsidated by TMV coat proteins, co-purified and be represented in mice injections. The possibility of sgRNA3 being used as mRNA templates has been considered, since sgRNA3 also contains eGFP sequence and contains a TMV 0a. However, from the numerous TEM images, it is apparent that the amount of sgRNA3 nanoparticles (~67nM) is not evident or a minority of the particles, and the majority nanoparticles are of full length (200nm) . Furthermore, from the previous literature, the non-replicating mRNA vaccination strategy has largely relied on extensive chemical modifications, additional use of adjuvants (43), and an *ex vivo* route to transinfect dendritic cells(44). In two studies using eGFP mRNA to transinfect dendritic cells, eGFP either degraded too rapidly due to the lack of additional targeting signals(46), or was expressed well in dendritic cells but failed to trigger dendritic cell maturation without using inducing agents(47). Overall, it is more likely that a functional replicase and a self-replicating viral RNA account for the bulk of the immune stimulation observed in this work, rather than translation from sgRNA3.

Several improvements can be made to the utility of TMV coat encapsidated RNA. In order to increase immune activation and greater CD4 T cell response, future optimization may include the use of other viruses with a replicase active at 37 degree, such as Nodamura virus (33). Peptide directed endosomal escape of nanoparticles (48-50) may also increase animal cell co-translational disassembly, and subsequent protein accumulation. In our study, eGFP was used to track viral expression of eGFP in plant and animal cells. Expression of a more potent immunogen (e.g., ovalbumin) with better characterized antigenicity should also improve measurement of both antibody and T cell immunogenicity after nanoparticle vaccination.

In conclusion, we were able to produce FHV RNA and TMV CP, in the same plant cell, resulting in assembly of rod shaped packaged RNA. These *in planta* produced nanoparticles were shown to induce an antigen-specific immunogenicity exceeding that of *in vitro* packaged RNA nanoparticles. Our next tasks are to investigate cellular localization of FHV RNA and TMV CP and to optimize heterologous virion assembly. We will also seek to target the hybrid virion nanoparticles to the correct compartment in the mammalian cell in order to facilitate TMV-CP virion disassembly and improved RNA 1 replication. Completion of these goals will answer basic virological questions of component trafficking, disassembly and replication in the process of optimizing vaccine production and potency.

References

1. Gutierro, I., Hernandez, R. M., Igartua, M., Gascon, A. R. and Pedraz, J. L. (2002) Influence of dose and immunization route on the serum Ig G antibody response to BSA loaded PLGA microspheres. Vaccine 20, 2181-2190.
2. Gutierro, I., Hernandez, R. M., Igartua, M., Gascon, A. R. and Pedraz, J. L. (2002) Size dependent immune response after subcutaneous, oral and intranasal administration of BSA loaded nanospheres. Vaccine 21, 67-77.
3. Dobrovolskaia, M. A. and McNeil, S. E. (2007) Immunological properties of engineered nanomaterials. Nature nanotechnology 2, 469-478.
4. McCormick, A. A., Reddy, S., Reinl, S. J., Cameron, T. I., Czerwinkski, D. K., Vojdani, F., Hanley, K. M., Garger, S. J., White, E. L., Novak, J., Barrett, J., Holtz, R. B., Tuse, D. and Levy, R. (2008) Plant-produced idiotype vaccines for the treatment of non-Hodgkin's lymphoma: safety and immunogenicity in a phase I clinical study. Proceedings of the National Academy of Sciences of the United States of America 105, 10131-10136.
5. Aires, K. A., Cianciarullo, A. M., Carneiro, S. M., Villa, L. L., Boccardo, E., Perez-Martinez, G., Perez-Arellano, I., Oliveira, M. L. and Ho, P. L. (2006) Production of human papillomavirus type 16 L1 virus-like particles by recombinant Lactobacillus casei cells. Applied and environmental microbiology 72, 745-752.
6. Huang, Z., Santi, L., LePore, K., Kilbourne, J., Arntzen, C. J. and Mason, H. S. (2006) Rapid, high-level production of hepatitis B core antigen in plant leaf and its immunogenicity in mice. Vaccine 24, 2506-2513.
7. Zhou, J., Sun, X. Y., Stenzel, D. J. and Frazer, I. H. (1991) Expression of vaccinia recombinant HPV 16 L1 and L2 ORF proteins in epithelial cells is sufficient for assembly of HPV virion-like particles. Virology 185, 251-257.
8. Diebold, S. S., Kaisho, T., Hemmi, H., Akira, S. and Reis e Sousa, C. (2004) Innate antiviral responses by means of TLR7-mediated recognition of single-stranded RNA. Science 303, 1529-1531.
9. Lund, J. M., Alexopoulou, L., Sato, A., Karow, M., Adams, N. C., Gale, N. W., Iwasaki, A. and Flavell, R. A. (2004) Recognition of single-stranded RNA viruses

564 by Toll-like receptor 7. Proceedings of the National Academy of Sciences of the
565 United States of America 101, 5598-5603.
566 10. Schwarz, K., Storni, T., Manolova, V., Didierlaurent, A., Sirard, J. C.,
567 Rothlisberger, P. and Bachmann, M. F. (2003) Role of Toll-like receptors in
568 costimulating cytotoxic T cell responses. European journal of immunology 33,
569 1465-1470.
570 11. Pogue, G. P., Lindbo, J. A., Garger, S. J. and Fitzmaurice, W. P. (2002) Making
571 an ally from an enemy: plant virology and the new agriculture. Annual review of
572 phytopathology 40, 45-74.
573 12. Liu, R., Vaishnav, R. A., Roberts, A. M. and Friedland, R. P. (2013) Humans
574 have antibodies against a plant virus: evidence from tobacco mosaic virus. PloS
575 one 8, e60621.
576 13. McCormick, A. A., Corbo, T. A., Wykoff-Clary, S., Palmer, K. E. and Pogue, G. P.
577 (2006) Chemical conjugate TMV-peptide bivalent fusion vaccines improve
578 cellular immunity and tumor protection. Bioconjugate chemistry 17, 1330-1338.
579 14. McCormick, A. A., Corbo, T. A., Wykoff-Clary, S., Nguyen, L. V., Smith, M. L.,
580 Palmer, K. E. and Pogue, G. P. (2006) TMV-peptide fusion vaccines induce cell-
581 mediated immune responses and tumor protection in two murine models.
582 Vaccine 24, 6414-6423.
583 15. Smith, M. L., Lindbo, J. A., Dillard-Telm, S., Brosio, P. M., Lasnik, A. B.,
584 McCormick, A. A., Nguyen, L. V. and Palmer, K. E. (2006) Modified tobacco mosaic
585 virus particles as scaffolds for display of protein antigens for vaccine
586 applications. Virology 348, 475-488.
587 16. Mallajosyula, J. K., Hiatt, E., Hume, S., Johnson, A., Jeevan, T., Chikwamba, R.,
588 Pogue, G. P., Bratcher, B., Haydon, H., Webby, R. J. and McCormick, A. A. (2013)
589 Single-dose monomeric HA subunit vaccine generates full protection from
590 influenza challenge. Human vaccines & immunotherapeutics 10, 586 - 595.
591 17. Fraile, A., Escriu, F., Aranda, M. A., Malpica, J. M., Gibbs, A. J. and Garcia-Arenal,
592 F. (1997) A century of tobamovirus evolution in an Australian population of
593 Nicotiana glauca. Journal of virology 71, 8316-8320.
594 18. Kemnade, J. O., Seethammagari, M., Collinson-Pautz, M., Kaur, H., Spencer, D.
595 M. and McCormick, A. A. (2014) Tobacco mosaic virus efficiently targets DC
596 uptake, activation and antigen-specific T cell responses in vivo. Vaccine 32,
597 4228-4233.
598 19. Koo, M., Bendahmane, M., Lettieri, G. A., Paoletti, A. D., Lane, T. E., Fitchen, J.
599 H., Buchmeier, M. J. and Beachy, R. N. (1999) Protective immunity against murine
600 hepatitis virus (MHV) induced by intranasal or subcutaneous administration of
601 hybrids of tobacco mosaic virus that carries an MHV epitope. Proceedings of the
602 National Academy of Sciences of the United States of America 96, 7774-7779.
603 20. Yin, Z., Nguyen, H. G., Chowdhury, S., Bentley, P., Bruckman, M. A., Miermont,
604 A., Gildersleeve, J. C., Wang, Q. and Huang, X. (2012) Tobacco mosaic virus as a
605 new carrier for tumor associated carbohydrate antigens. Bioconjugate chemistry
606 23, 1694-1703.

607 21. Smith, M. L., Corbo, T., Bernales, J., Lindbo, J. A., Pogue, G. P., Palmer, K. E. and
608 McCormick, A. A. (2007) Assembly of trans-encapsidated recombinant viral
609 vectors engineered from Tobacco mosaic virus and Semliki Forest virus and
610 their evaluation as immunogens. Virology 358, 321-333.
611 22. Lundstrom, K. (2003) Semliki Forest virus vectors for gene therapy. Expert
612 opinion on biological therapy 3, 771-777.
613 23. Mahraj, P. D., Mallajosyula, J. K., Lee, G., Thi, P., Zhou, Y., Kearney, C. M. and
614 McCormick, A. A. ((accepted, 2014)) Nanoparticle encapsidation of Flock House
615 virus by auto assembly of Tobacco Mosaic virus coat protein. International
616 Journal of Molecular Sciences.
617 24. Johnson, K. L. and Ball, L. A. (1999) Induction and maintenance of
618 autonomous flock house virus RNA1 replication. Journal of virology 73, 7933-
619 7942.
620 25. Selling, B. H., Allison, R. F. and Kaesberg, P. (1990) Genomic RNA of an insect
621 virus directs synthesis of infectious virions in plants. Proceedings of the National
622 Academy of Sciences of the United States of America 87, 434-438.
623 26. Price, B., Roeder, M. and Ahlquist, P. (2000) DNA-Directed Expression of
624 Functional Flock House Virus RNA1 Derivatives in Saccharomyces cerevisiae,
625 Heterologous Gene Expression, and Selective Effects on Subgenomic mRNA
626 Synthesis. Journal of virology 74, 11724–11733.
627 27. Lindbo, J. A. (2007) High-efficiency protein expression in plants from
628 agroinfection-compatible Tobacco mosaic virus expression vectors. BMC
629 biotechnology 7, 52.
630 28. Turner, D. R. and Butler, P. J. (1986) Essential features of the assembly origin
631 of tobacco mosaic virus RNA as studied by directed mutagenesis. Nucleic acids
632 research 14, 9229-9242.
633 29. Liu, Z. and Kearney, C. M. (2010) An efficient Foxtail mosaic virus vector
634 system with reduced environmental risk. BMC biotechnology 10, 88.
635 30. Dasgupta, R., Cheng, L. L., Bartholomay, L. C. and Christensen, B. M. (2003)
636 Flock house virus replicates and expresses green fluorescent protein in
637 mosquitoes. Journal of General Virology 84, 1789-1797.
638 31. Price, B. D., Ahlquist, P. and Ball, L. A. (2002) DNA-Directed Expression of an
639 Animal Virus RNA for Replication-Dependent Colony Formation in
640 Saccharomyces cerevisiae. Journal of virology 76, 1610-1616.
641 32. Scholthof, H. B. (2006) The Tombusvirus-encoded P19: from irrelevance to
642 elegance. Nat Rev Microbiol 4, 405-411.
643 33. Ball, L. A., Amann, J. M. and Garrett, B. K. (1992) Replication of Nodamura
644 Virus after Transfection of Viral-Rna into Mammalian-Cells in Culture. Journal of
645 virology 66, 2326-2334.
646 34. Hwang, D. J., Roberts, I. M. and Wilson, T. M. (1994) Expression of tobacco
647 mosaic virus coat protein and assembly of pseudovirus particles in Escherichia
648 coli. Proceedings of the National Academy of Sciences of the United States of
649 America 91, 9067-9071.

650 35. Sleat, D. E., Gallie, D. R., Watts, J. W., Deom, C. M., Turner, P. C., Beachy, R. N.
651 and Wilson, T. M. (1988) Selective recovery of foreign gene transcripts as virus-
652 like particles in TMV-infected transgenic tobaccos. Nucleic acids research 16,
653 3127-3140.
654 36. Sacher, R., French, R. and Ahlquist, P. (1988) Hybrid brome mosaic virus
655 RNAs express and are packaged in tobacco mosaic virus coat protein in vivo.
656 Virology 167, 15-24.
657 37. Annamalai, P., Rofail, F., Demason, D. A. and Rao, A. L. (2008) Replication-
658 coupled packaging mechanism in positive-strand RNA viruses: synchronized
659 coexpression of functional multigenome RNA components of an animal and a
660 plant virus in Nicotiana benthamiana cells by agroinfiltration. Journal of virology
661 82, 1484-1495.
662 38. Rao, A. L. (2006) Genome packaging by spherical plant RNA viruses. Annual
663 review of phytopathology 44, 61-87.
664 39. Wilson, T. M. and McNicol, J. W. (1995) A conserved, precise RNA
665 encapsidation pattern in Tobamovirus particles. Archives of virology 140, 1677-
666 1685.
667 40. Abel, P. P., Nelson, R. S., De, B., Hoffmann, N., Rogers, S. G., Fraley, R. T. and
668 Beachy, R. N. (1986) Delay of disease development in transgenic plants that
669 express the tobacco mosaic virus coat protein gene. Science 232, 738-743.
670 41. Lindenbach, B. D., Sgro, J. Y. and Ahlquist, P. (2002) Long-Distance Base
671 Pairing in Flock House Virus RNA1 Regulates Subgenomic RNA3 Synthesis and
672 RNA2 Replication. Journal of virology 76, 3905-3919.
673 42. Sztuba-Solinska, J., Stollar, V. and Bujarski, J. J. (2011) Subgenomic messenger
674 RNAs: mastering regulation of (+)-strand RNA virus life cycle. Virology 412, 245-
675 255.
676 43. Phua, K. K., Nair, S. K. and Leong, K. W. (2014) Messenger RNA (mRNA)
677 nanoparticle tumour vaccination. Nanoscale 6, 7715-7729.
678 44. Weiner, D. B. (2013) RNA-based vaccination: sending a strong message.
679 Molecular therapy : the journal of the American Society of Gene Therapy 21, 506-
680 508.
681 45. Eckerle, L. D., Albarino, C. G. and Ball, L. A. (2003) Flock House virus
682 subgenomic RNA3 is replicated and its replication correlates with
683 transactivation of RNA2. Virology 317, 95-108.
684 46. Bonehill, A., Heirman, C., Tuyaerts, S., Michiels, A., Breckpot, K., Brasseur, F.,
685 Zhang, Y., van der Bruggen, P. and Thielemans, K. (2004) Messenger RNA-
686 Electroporated Dendritic Cells Presenting MAGE-A3 Simultaneously in HLA Class
687 I and Class II Molecules. The Journal of Immunology 172, 6649-6657.
688 47. Van Tendeloo, V. F., Ponsaerts, P., Lardon, F., Nijs, G., Lenjou, M., Van
689 Broeckhoven, C., Van Bockstaele, D. R. and Berneman, Z. N. (2001) Highly
690 efficient gene delivery by mRNA electroporation in human hematopoietic cells:
691 superiority to lipofection and passive pulsing of mRNA and to electroporation of
692 plasmid cDNA for tumor antigen loading of dendritic cells. Blood 98, 49-56.

48. Tkachenko, A. G., Xie, H., Coleman, D., Glomm, W., Ryan, J., Anderson, M. F., Franzen, S. and Feldheim, D. L. (2003) Multifunctional gold nanoparticle-peptide complexes for nuclear targeting. J Am Chem Soc 125, 4700-4701.
49. Oliveira, S., van Rooy, I., Kranenburg, O., Storm, G. and Schiffelers, R. M. (2007) Fusogenic peptides enhance endosomal escape improving siRNA-induced silencing of oncogenes. International journal of pharmaceutics 331, 211-214.
50. Erazo-Oliveras, A., Muthukrishnan, N., Baker, R., Wang, T.-Y. and Pellois, J.-P. (2012) Improving the Endosomal Escape of Cell-Penetrating Peptides and Their Cargos: Strategies and Challenges. Pharmaceuticals 5, 1177-1209.

Figure Legends

FIG 1 FHV viral vector constructs for expression in mammalian cells. (A) Two constructs, C2 and C4, differing in the insertion site for eGFP. B2, FHV silencing suppressor; Rbz, HDV ribozyme for precise viral RNA 3' end excision. (B) Expression of T7/FHV-C2-GFP (left) and T7/FHV-C4-GFP (right) in BHK21 cells.

FIG 2 FHV viral vector constructs for expression in plants. The C2 and C4 constructs from Figure 1 were provided with the 35S plant expression promoter and the TMV origin of assembly (Oa) to allow for encapsidation. (A) In the C2 series, TMV-Oa was added at different positions in C2-o1, and -o2, and in -o3 the eGFP native C terminal stop codon was preserved. B2' stands for the B2 ORF C-terminal remaining after eGFP insertion. (B) The C4-2sg has a duplicated subgenomic promoter to express unfused versions of eGFP and B2 silencing suppressor. The eGFP ORF is between the duplicated

719 subgenomic promoters in C4-2sg, but follows the final subgenomic promoter
720 in 2sg2 construct. The 2sg2 constructs retain the B2 C-terminus (B2'')
721 following the eGFP ORF to mimic the 3' end of the native FHV. (C) The
722 FECT/TMVCP construct and the JL6/p19 were used as co-agroinoculants
723 and provided coat protein and silencing suppressor, respectively.
724
725 **FIG 3** eGFP expression from constructs from Figure 2. Agroinoculated leaves
726 of *Nicotiana benthamiana* were examined, 7 dpi, under blue light with visible
727 light to outline leaf shape. 35S/FHV-C2 inoculated alone or with p19 silencing
728 suppressor. FECT-eGFP is general high expression positive control. F1DI (+/-
729 p19) is a positive control for FHV/GFP expression and comprises FHV RNA1
730 plus a defective interfering construct of RNA2. All other inoculations included
731 p19 unless otherwise mentioned. 2sg2KSS construct is included in the
732 supplementary data. All other designations as in Figure 2.
733
734 **FIG 4** eGFP expression in plants by FHV constructs and in 1-step and 2-step
735 inoculation procedures. (A) eGFP fluorometry of *N. benthamiana*
736 agroinoculated with various FHV constructs. p19, mock inoculation with p19
737 only; FECT-eGFP, high expression positive control; 1-step and 2-step, co-
738 agroinoculation or delayed TMVCP agroinoculation. Four replicates each
739 treatment, except 15 replicates for 1-step and 2-step treatments. (B) eGFP

740 expression compared in 1-step and 2-step agroinoculation procedures. FHV-
741 C2-o3 without any FECT-TMV was also inoculated as a control.
742
743 **FIG 5** Expression of TMV CP by FECT plant viral vector. Lane a, FECT
744 expressing TMV CP; Lane b, TMV vector JL24 (23) expressing CP and
745 eGFP. Both agroinoculations in *N. benthamiana* included p19 silencing
746 suppressor. Far left lane: protein marker (NEB # P7708) with sizes in kDa
747 indicated.
748
749 **FIG 6** Co-infection of plant cells by FHV and FECT viral vectors. (A) *N.*
750 *benthamiana* plants were agroinoculated with p19 plus (left to right)
751 35S/FHVC2-o3/GFP, FECT/DsRed or both vectors. (B) Protoplasts made
752 from 4 dpi leaves coagroinoculated with FHV-eGFP/FECT-DsRed (right leaf
753 in (A)) were visualized for eGFP and DsRed fluorescence, showing the
754 majority of the FHV-eGFP infected cells were also infected with FECT.
755
756 **FIG 7** TEM of *in vitro* and *in planta* produced nanoparticles. (A) *In vitro*
757 assembled FHVOa. (B) *In vitro* assembled SFVOa (C) *in planta* assembled
758 FHV-C2-o3 (CP provided by FECT/TMVCP). 100 nm bars indicated.
759
760 **FIG 8** *In vivo* analysis of FHV vaccine potency. Balb/C Mice (n = 3) were
761 vaccinated 3 times, two weeks apart with indicated amounts (15 or 30 μg

762 protein) of TMV encapsidated FHV-eGFP, produced either *in vitro* by mixing
763 RNA and coat protein, or *in planta* by co-expression of RNA and coat protein
764 after agroinfiltration. PBS was used as a negative control, and *in vitro*
765 encapsidated SFV-eGFP or 15ug of eGFP protein was used as a positive
766 control. ELISA analysis was used to determine anti-eGFP IgG titers on sera
767 collected at 10 d after either vaccine 2 (pV2) or after vaccine 3 (pV3). Titers
768 were measured against a known quantity of anti-eGFP standard (Vector
769 labs), and shown as mean +/- SEM using GraphPad Prism. Statistical
770 analysis of differences between PBS and vaccine groups after vaccine 3 was
771 evaluated by one-tailed t-test. The asterisk indicates statistically significant
772 difference from PBS control.
773
774
775
776
777
778
779
780
781
782
783

784

A.

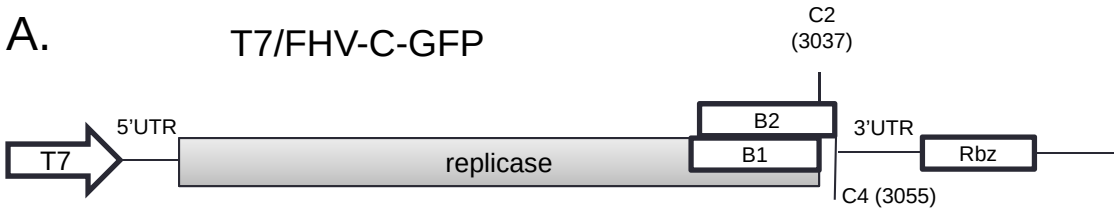

B.

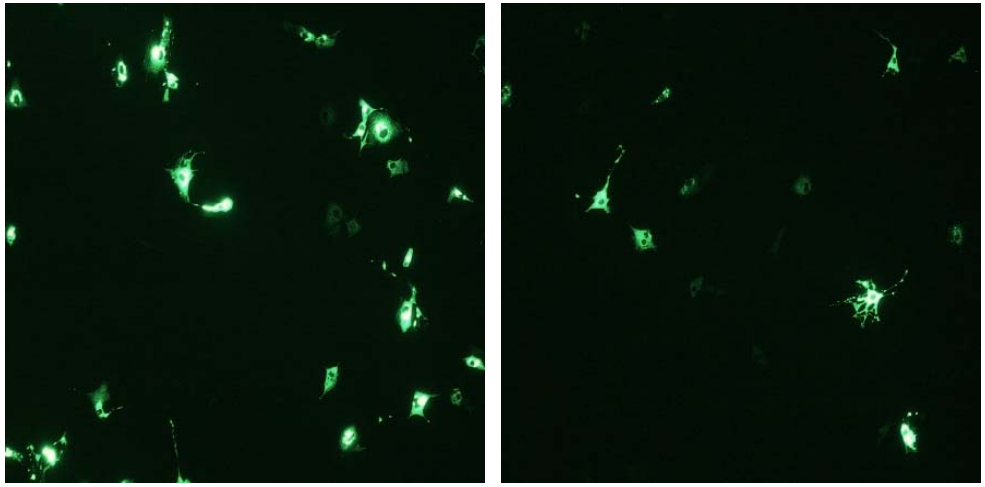

Figure 1

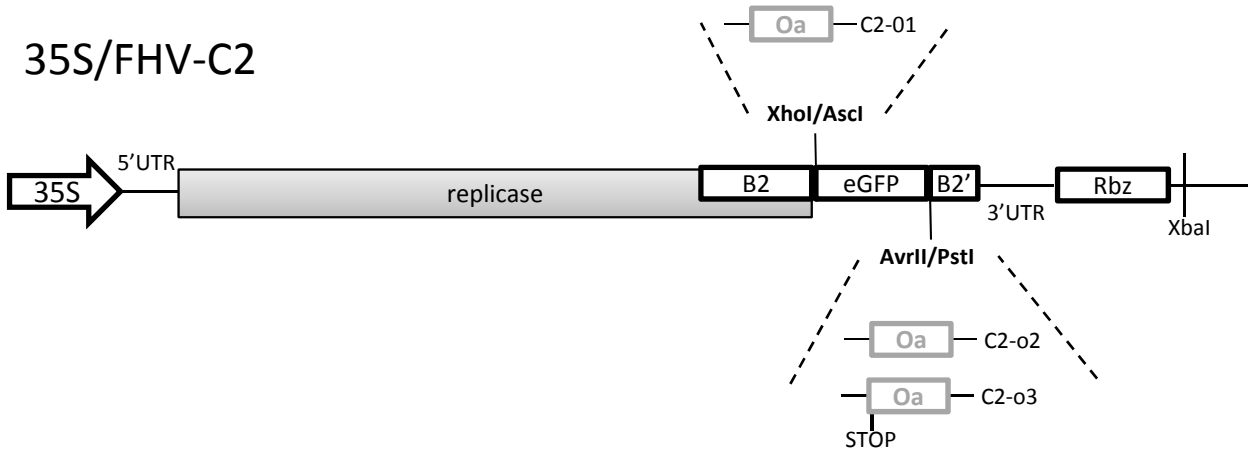
35S/FHV-C2
Oa
C2-01
XhoI/AscI
5'UTR
35S
replicase
B2
eGFP
B2'
3'UTR
Rbz
XbaI
AvrII/PstI
Oa
C2-o2
Oa
C2-o3
STOP

Figure 2A

35S/FHV-C4-2sg

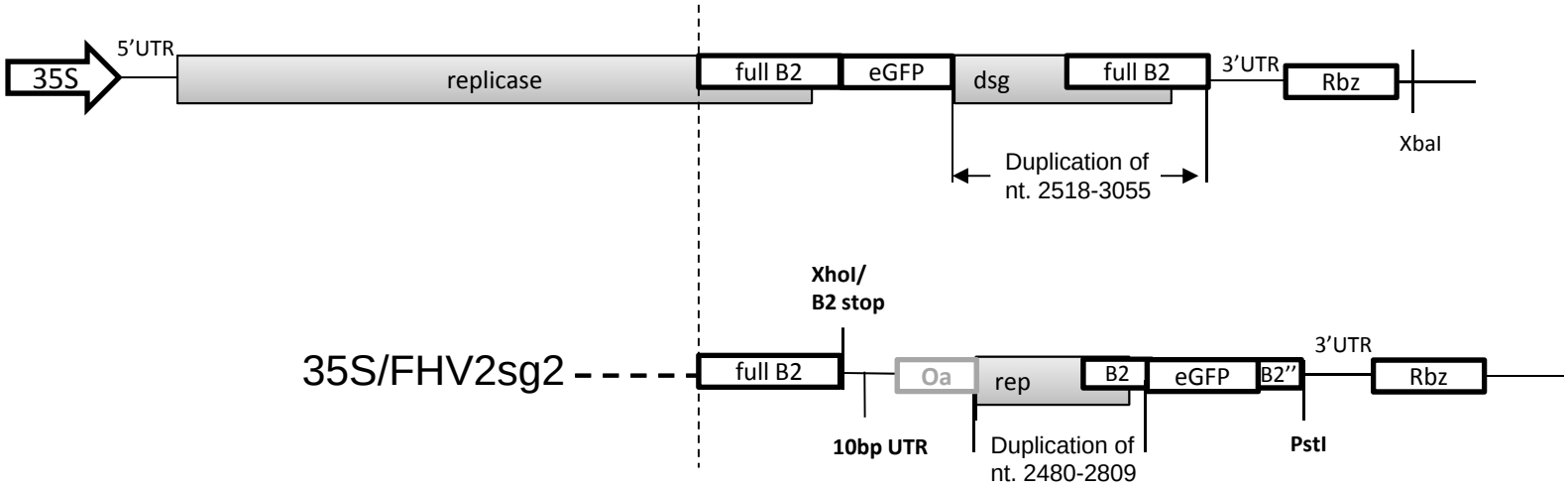

Figure 2B

FECT/TMVCP

JL6/p19

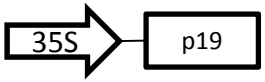

Figure 2C

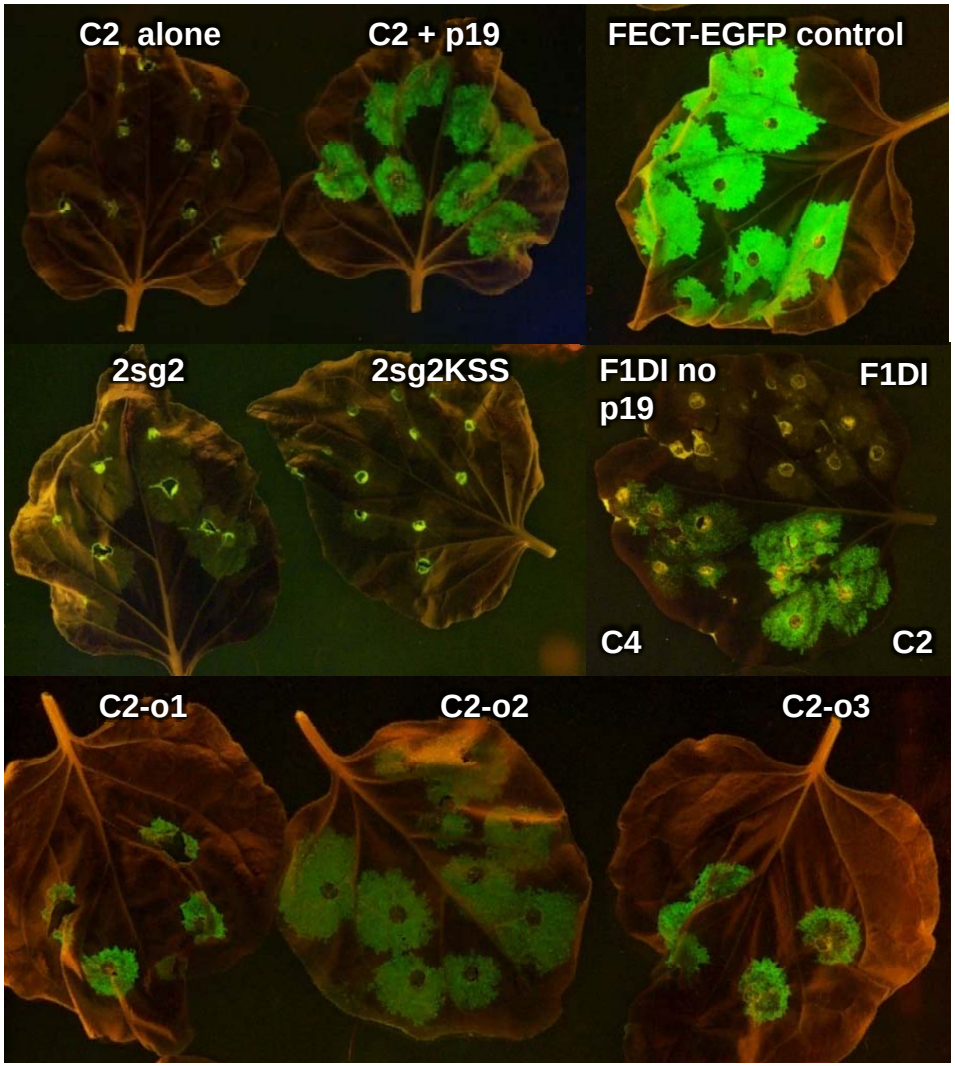
C2 alone
C2 + p19
FECT-EGFP control
2sg2
2sg2KSS
F1DI no p19
F1DI
C4
C2
C2-o1
C2-o2
C2-o3

Figure 3

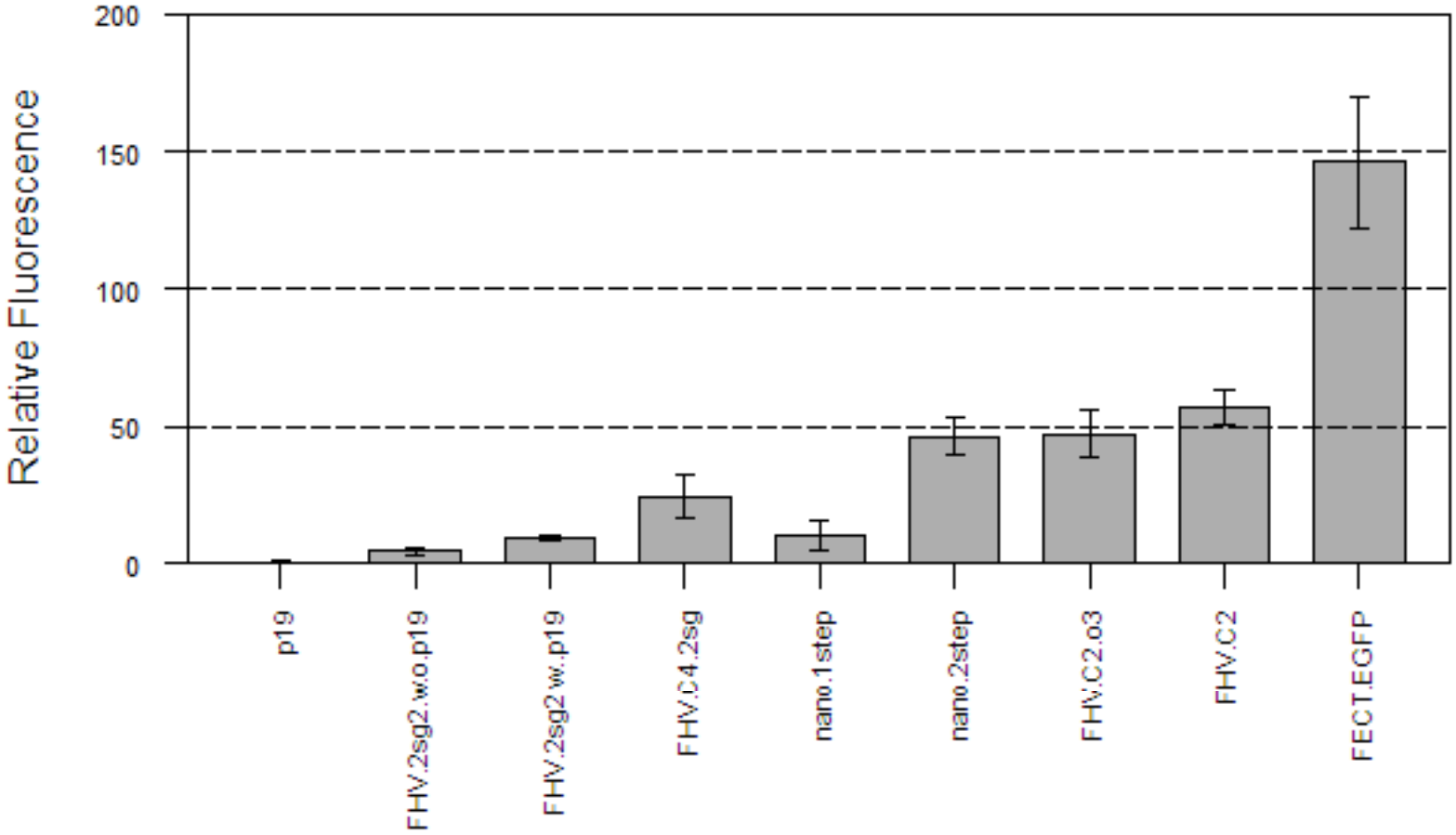
Relative Fluorescence
200
150
100
50
0
p19
FHV.2sg2.w.o.p19
FHV.2sg2.w.p19
FHV.C4.2sg
nano.1step
nano.2step
FHV.C2.o3
FHV.C2
FECT.EGFP

Figure 4A

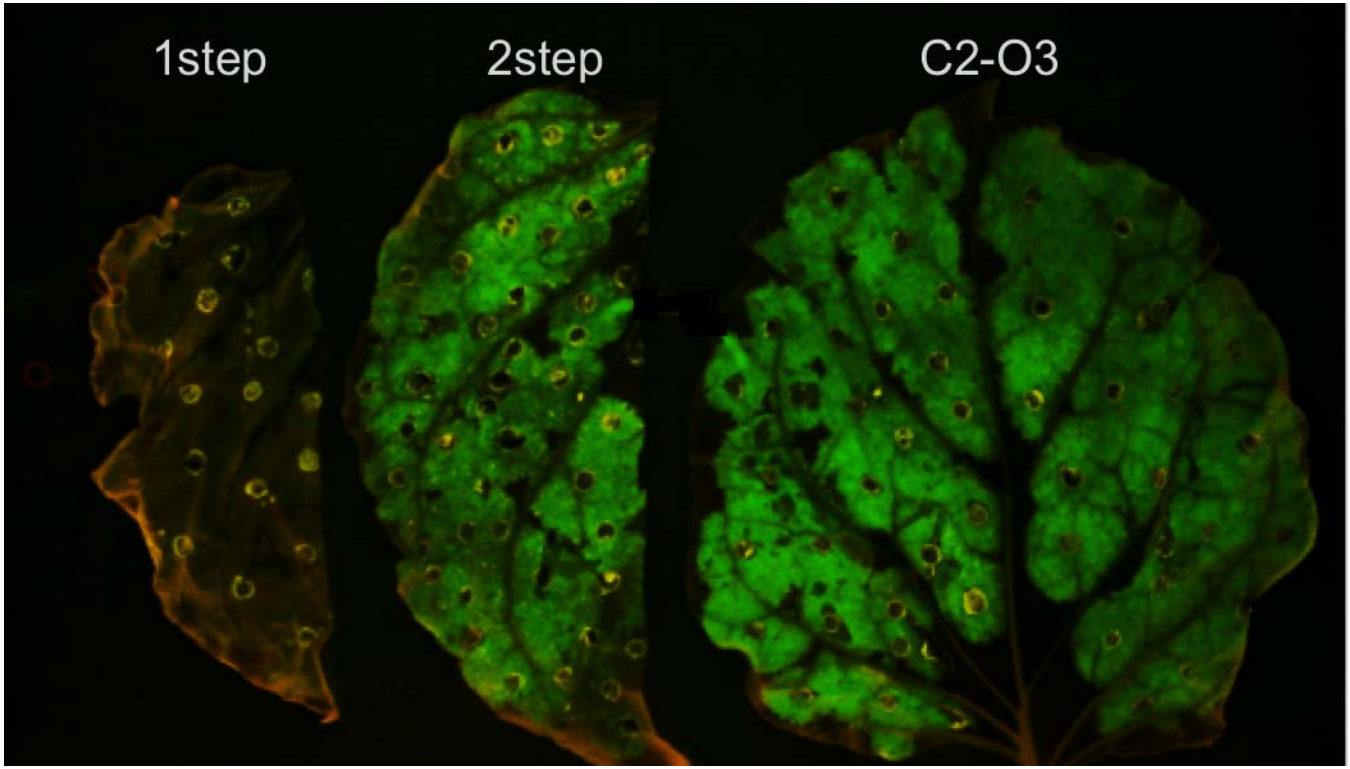

Figure 4B

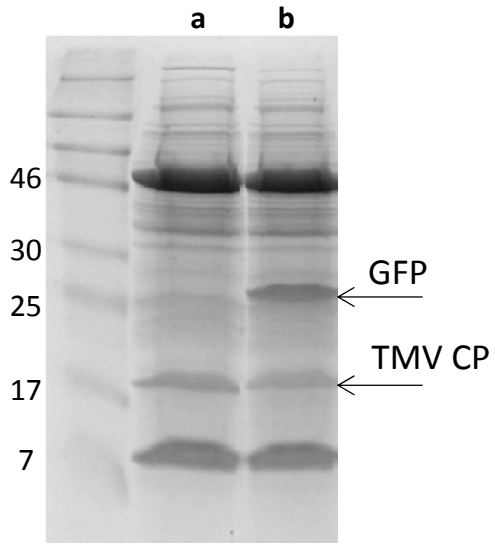

Figure 5

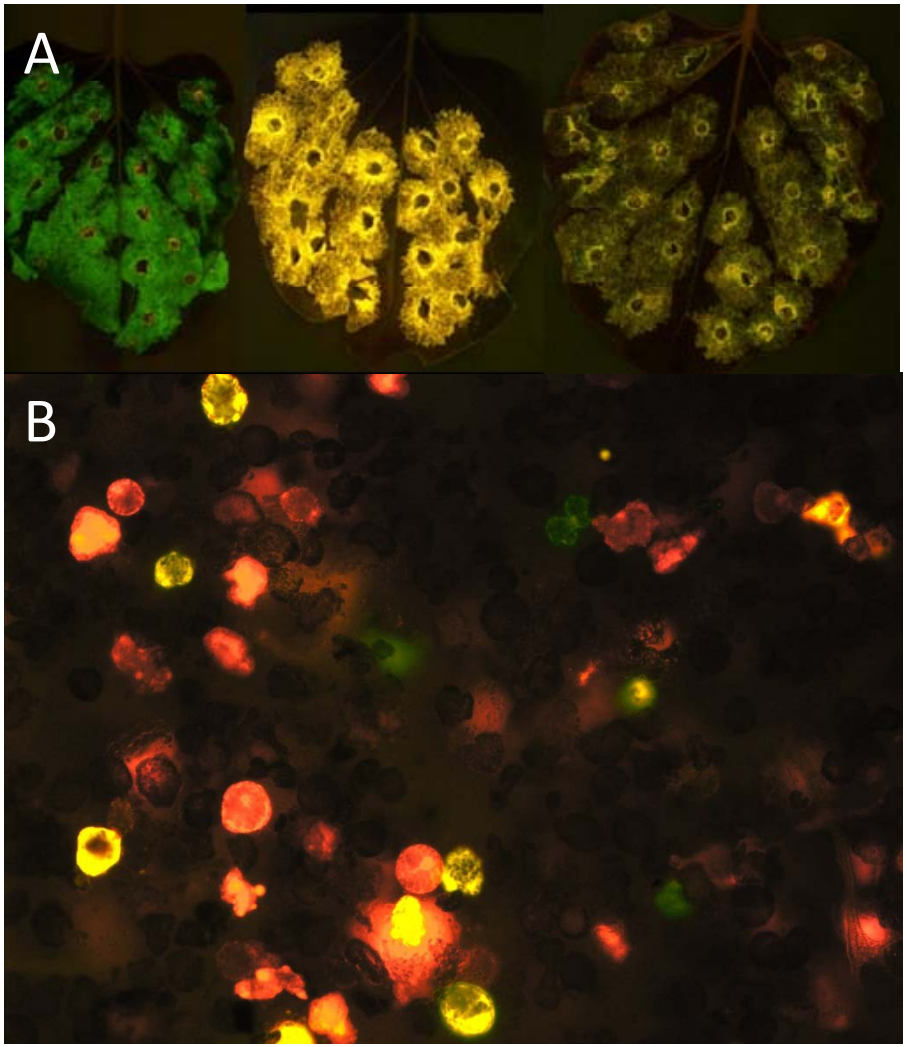

Figure 6

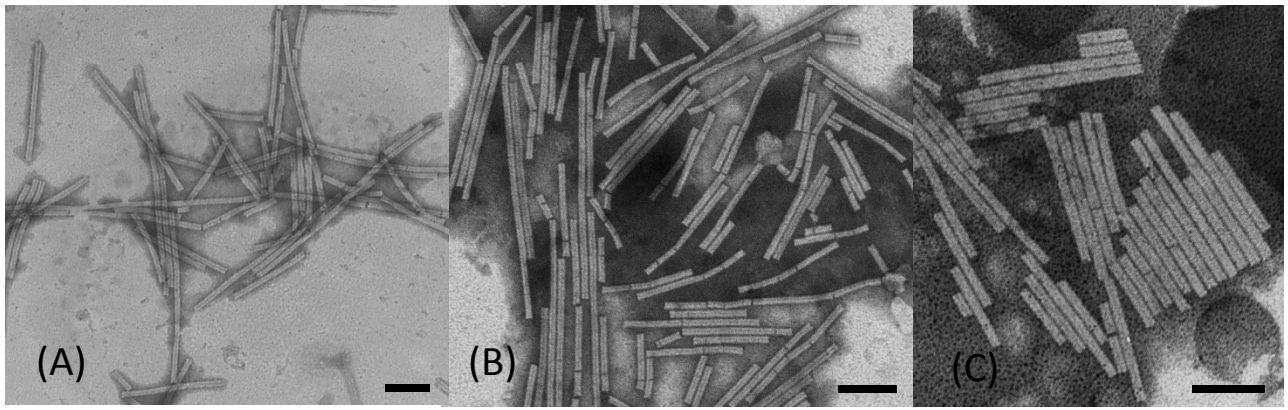

Figure 7

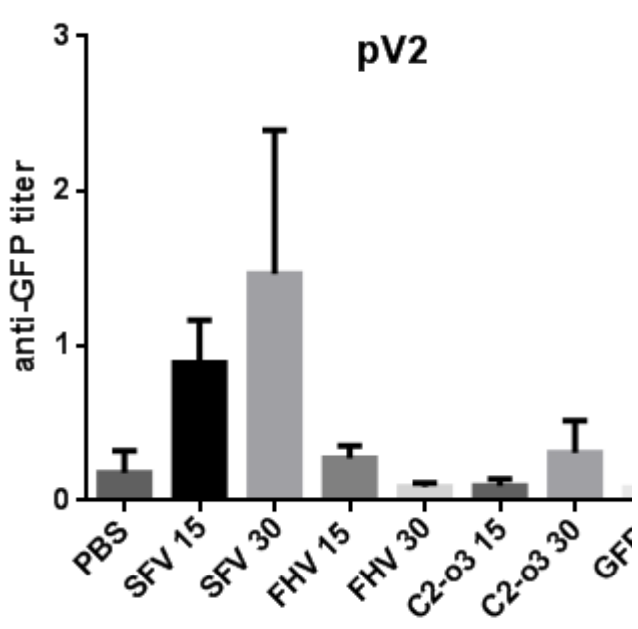

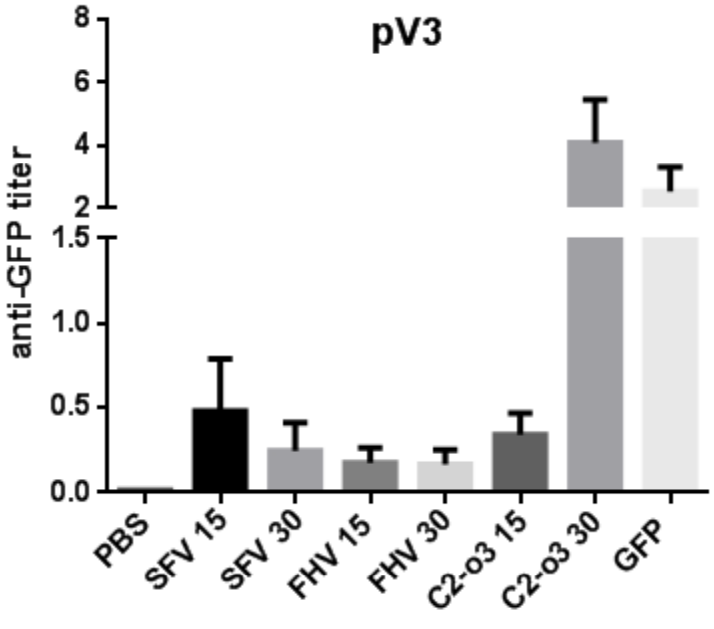

one tailed t-test vs PBS:
SFV 15 p=0.224
SFV 30 p=0.116
FHV 15 p=0.104
FHV 30 p=0.110
C2-o3 15 p=0.063
*C2-o3 30 p=0.048
*GFP p=0.047

Figure 8

FHV2sg2KSS

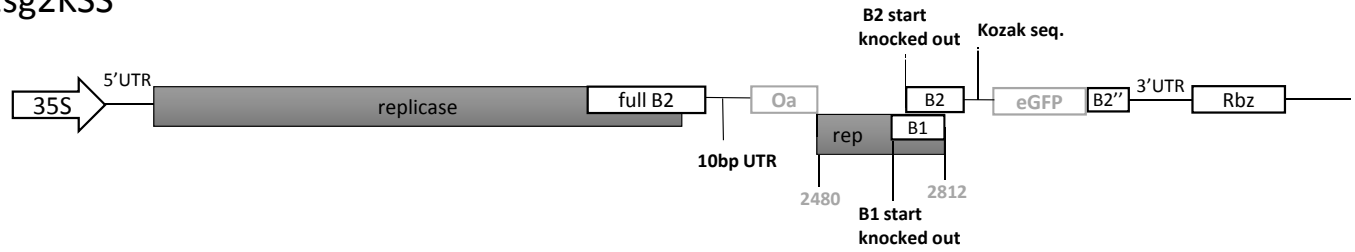

Suppl. Fig 1: In seek to further aid eGFP expression, a 35S/FHV-2sg2KSS construct was built, in which the B1 and B2 start codons were knocked out and an ATG with strong Kozak context (CCACC ATG) was placed at the start of the eGFP ORF, resulting in an eGFP/B2 fusion with only a short B2 portion C-terminal to the eGFP.

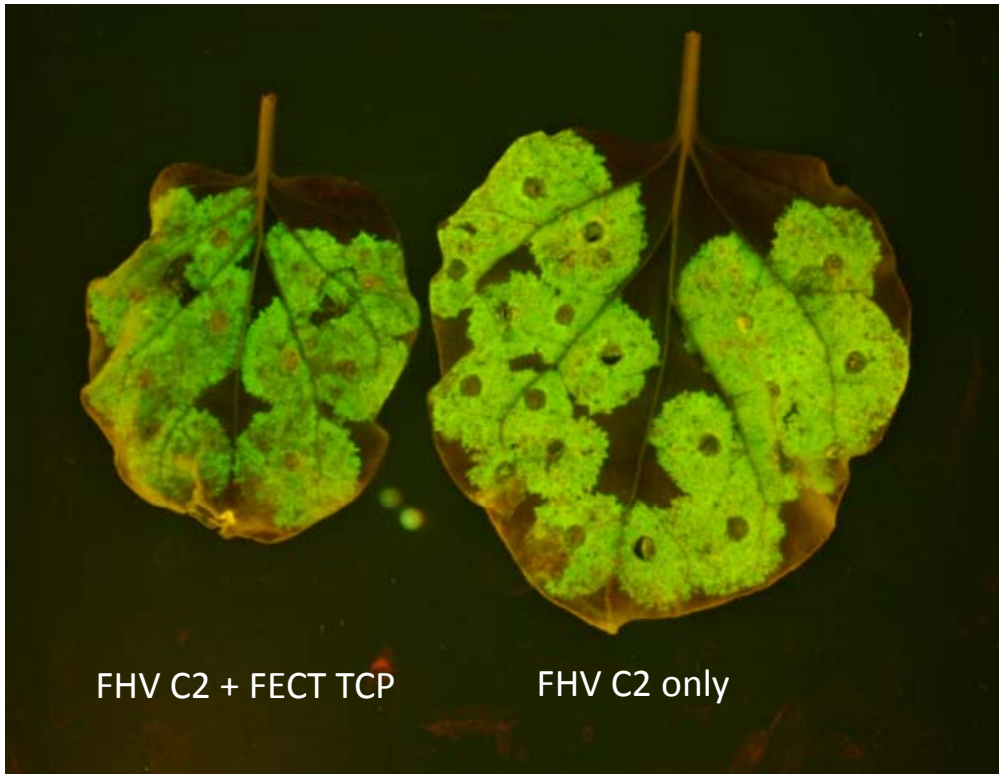

Suppl. Fig 2: In order to determine whether FECT virus will interfere with FHV replication in planta, FHVC2/GFP lacking the Oa sequence was co-inoculated with FECT-TCP and compared with FHVC2/GFP in the absence of FECT-TCP. Fluorescence was similar in the presence (left) or absence (right) of FECT coinfection. This confirmed the reduction of fluorescence by coinfection with FHVC2/GFP containing the TMV Oa and FECT-TCP expressing coat protein is due to the hypothesized classical coat protein resistance. All experiments were carried out with p19 co-inoculation